J. Mater. Chem. B, 5, 6776-6785, 2017

ARTICLE

Poly(amidoamine) dendrimers grafted on electrospun poly(acrylic acid)/poly(vinyl alcohol) membranes for host-guest encapsulation of the antioxidant thymol

Georgiana Amariei[a], Karina Boltes[a], Pedro Letón[a], Isabel Iriepa[b], Ignacio Moraleda[b], Roberto Rosal[a,†]

[a] Department of Chemical Engineering, University of Alcalá, E-28871 Alcalá de Henares, Madrid, Spain. E-mail: roberto.rosal@uah.es
[b] Department of Organic Chemistry and Inorganic Chemistry, School of Biology, Environmental Sciences and Chemistry, University of Alcalá, E-28871 Alcalá de Henares, Madrid, Spain
† Electronic supplementary information (ESI) available at the end of this file: Computational images of thymol molecules associated with dendrimers.

Abstract
Amino-terminated fifth generation poly(amidoamine) dendrimer molecules (PAMAM G5-NH_2) were grafted onto the surface of poly(acrylic acid)/poly(vinyl alcohol) (PAA/PVA) electrospun fibres with the purpose of creating a host-guest architecture for the controlled delivery of the natural antioxidant thymol. The nanofibers were stabilized by esterification crosslinking to produce a water insoluble non-woven membrane. The functionalization with PAMAM G5-NH_2 led to dendrimer loadings in the 7.4 x 10^{-7} - 2.25 x 10^{-6} mol dendrimer/g membrane range. The resulting materials were characterized using SEM, ATR-FTIR and surface ζ-potential measurements. The loading capacity for thymol reached 2.5 x 10^{-4} mol thymol/g membrane. The membranes were tested for thymol release in different aqueous and non-aqueous food simulants. Computational modelling was used to get a further insight into the host-guest association of thymol and PAMAM G5-NH_2 molecules through docking studies. For this purpose, we examined the molecular level details of the dendrimer-guest complex, calculated the number of included or attached molecules, the exact location of thymol in host-guest complexes and the local environment around the thymol molecules. Docking studies showed that PAMAM-G5-NH_2 dendrimers can encapsulate thymol molecules through hydrophobic interactions and hydrogen bonding. The maximum amount of thymol molecules theoretically encapsulated was 16, while another 25 could be hosted at the dendrimer surface through interaction with the outer part or the dendritic branches. The experimental value was 37 ± 5 consistent with theoretical predictions.

Introduction

Electrospinning is a simple and cost-effective method for producing fibres below the micron size. Many polymeric nanofibres have been already produced using this technique for a variety of application areas [1]. In electrospinning, a thin jet of dissolved or molten polymer is accelerated due to the electric field forced by a high voltage source to a collector electrode. During the whipping-like path to the collector, the solvent evaporates or the polymer solidifies yielding an ordered array of fibres or a disordered nonwoven membrane depending on the collector geometry [2]. Electrospun materials can be used to create carriers for insoluble molecules by simple dispersion into the polymeric matrices [3]. Many systems based on biodegradable and non-biodegradable polymers have been proposed based on this idea [4]. The release of hosted molecules can be diffusion controlled or triggered by means of polymers responsive to environment variables like pH [5]. The critical aspects for the formulation of electrospun carriers are the compatibility between drug and polymer and the solubility of both in the electrospinning solution [6]. If the compatibility between drug and polymer does not allow direct co-electrospinning, other possibilities exist such as coaxial electrospinning, which allows one-step encapsulation of labile or non-solvent compatible compounds without using solvents or emulsifiers [7]. Another possibility for electrospun fibers in drug delivery applications are host-guest inclusion complexes such as those prepared from cyclodextrins [8].

Dendrimers are nano-sized, radially symmetric, essentially monodispersed hyper-branched polymers consisting of a central core, from which radially branched monomers grow forming successive shells referred to as generations (denoted by G) [9]. Dendrimers are globular molecules the outer core of which consists of a compact layer of surface end-groups that can be easily functionalized [10]. The useful properties of dendrimers include chemical stability, low viscosity and high solubility, thank to which they have been proposed for a number of applications that include catalytic, sensing, environmental and biomedical uses [11]. The branched structure of dendrimers leads to formation of relatively large internal cavities, which can offer unique microenvironments allowing

different chemical species to be accommodated within [12]. Overall, dendrimers exhibit a molecular architecture capable of interacting with a wide variety of molecules either by encapsulation, which generally involves electrostatic, hydrophobic and hydrogen bond interactions, or by surface attachment by electrostatic interactions or covalent bonding. The interacting mode of the ligands depends on the structure of dendritic core and ligands but also on pH because the dendrimers can undergo pH responsive conformational changes upon protonation of internal and core moieties [13]. The host-guest capacity of dendrimers arising from their internal cavities and surface structure, makes them very attractive for creating drug delivery materials [14, 15].

Thymol (5-methyl-2-isopropylphenol) is a natural monoterpene phenol derivative of cymene found in thyme extracts with natural antioxidant and antimicrobial properties. Its use is supported by the fact that thymol is listed by the Food and Drug Administration (FDA) as food additive on the GRAS (Generally recognized as Safe) list. The use of thymol and other natural extracts faces the problems of the ease of degradation of many of extracted compounds, their limited water solubility and the short term bioactivity due to their volatile character [16]. Thymol has been included in different kinds of films for active packaging to extend the shelf life of food products [17-19]. The hydrophobicity of thymol has been overcome by incorporating it into submicron emulsions with and without a carrier oil [20]. The encapsulation of thymol in water-dispersible zein nanocarriers has also been proposed for ensuring sustained activity in aqueous medium [21]. Another important feature of encapsulated systems is that the inclusion of hydrophobic antioxidant compounds may enhance the antioxidant performance due to the protective effect offered by host-guest architectures against the degradation of the active molecules [22].

In this work, we prepared electrospun membranes modified with amino terminated poly(amidoamine) fifth generation dendrimers (PAMAM G5-NH_2) for its use as thymol carriers using the host-guest capacity of dendrimers. The dendrimers were grafted to electrospun fibers made of poly(acrylic acid) (PAA) and polyvinyl alcohol (PVA). PAA and PVA are non-toxic water-soluble polymers that can be electrospun without organic solvents that produce insoluble PAA/PVA membranes by crosslinking esterification [23]. Poly(vinyl alcohol) and poly(acrylic acid) are two important materials that can be used to form hydrogels for tissue engineering scaffolds and for the design of drug delivery systems [24]. Hydrogel forming polymers are desired to be non-toxic to the cells they are in contact while serving as scaffold or delivering active compounds and to the surrounding tissues. The toxicity usually comes from the release of toxic leachable compounds or unreacted cross-linking agents [25]. Most stable hydrogels are non-toxic and do not induce immune responses when properly prepared, but they do need to be modified in order to promote cellular adhesion if serving as scaffold. In this regard, PVA has been modified with the fibronectin protein to promote functionality[26]. Poly(acrylic acid), however, has been shown to depress cell growth due to its acidic environment [27]. Cell adhesion and growth has been enhanced in this case by immobilizing collagen on the PAA surface [28]. Another interesting feature of PAA/PVA fibres is the intrinsic antimicrobial activity of poly(acrylic acid) polymers, which has been recently studied demonstrating that the binding by PAA of the divalent cations that stabilize prokaryotic membranes was the cause for the impairment of bacterial cells in contact with PAA/PVA membranes [29] [23]. Computational modelling was used to get a further insight into the host-guest association of thymol and PAMAM G5-NH_2 molecules through docking studies. Our contribution emphasizes the nature and relative strength of the intermolecular interactions responsible for the dendrimer-target interactions and binding mechanisms. Despite recent advances in cheminformatics, the amount of molecular modelling research is limited due to the lack of understanding of interactions at the atomic level. Computer strategies have the potential to minimize laborious and expensive laboratory experiments by guiding experimentation based on rational design. For this purpose, we examined the molecular level details of the dendrimer-guest complex, calculated the number of included or attached molecules, the exact location of thymol in host-guest complexes and the local environment around the thymol molecules. The results were compared with the experimental loading capacity of membranes grafted with PAMAM G5-NH_2.

Experimental

Chemicals

Poly(vinyl alcohol) (PVA, MW 89-98 kDa, 99+% hydrolysed) and poly(acrylic acid) (PAA, MW 450 kDa) from Sigma Aldrich were used to prepare the polymeric fibrous matrix. PAMAM dendrimer generation 5 (PAMAM G5-NH_2), 4.57 wt% solution in water, was purchased from Dendritech (Midland, MI, USA). N,N-dicyclohexylcarbodiimide (DCC, MW 206.33, 99%) and thymol (99+%) were obtained from Sigma Aldrich. N,N-dimethylformamide (DMF, 99%) and absolute ethanol (EtOH) were obtained from Scharlab (Spain). Ultrapure water (Milipore Mili-Q System) with a resistivity of at least 18 MΩ cm at 25 °C was used during the processes of fibre production and modification.

Preparation of electrospun fibres

The PAA/PVA electrospun fibres used to attach dendrimers were prepared as described elsewhere [23]. Briefly, the spinning solution was a polymeric mixture of 8 wt% PAA and 15 wt% PVA in ultrapure water. Two formulations with a final PAA/PVA weight ratio of 83:17 and 35:65 were produced to study the effect of different amounts of carboxylic acid groups on the functionalization process. The formulations refer to the weight ratio of PAA and PVA, 83/17 meaning 83 wt.% PAA and 17 wt% PVA in the final, solvent free, material. The solutions were stirred for 2h at 25 °C and degassed before electrospinning. The solution was drawn into a 5 mL syringe equipped with a

DOI: 10.1039/C7TB01498H

Table 1. PAMAM G5-NH_2-functionalized membranes prepared in this work

Membrane	PAA/PVA formulation (w/w)	-COOH amount (mmol COOH /g membrane)	PAMAM-G5-NH_2 amount used (mmol G5/mg membrane)	PAMAM-G5-NH_2 content (mmol G5/mg membrane)
83/17 (Neat)	83/17	12.5 ± 0.7	-	-
G5(-)@83/17			1.15×10^{-6}	$1.06 \times 10^{-6} \pm 4.1 \times 10^{-7}$
G5(+)@83/17			2.31×10^{-6}	$2.25 \times 10^{-6} \pm 3.0 \times 10^{-7}$
35/65 (Neat)	35/65	7.9 ± 0.3	-	-
G5(-)@35/65			1.15×10^{-6}	$7.4 \times 10^{-7} \pm 1.5 \times 10^{-7}$
G5(+)@35/65			2.31×10^{-6}	$1.55 \times 10^{-6} \pm 1.6 \times 10^{-7}$

23-gauge stainless steel blunt-tip needle and electrospun using the following parameters: voltage 23 kV, working distance 23 cm, flow rate 0.8 mL/h, RH 40%, temperature 25 °C. A drum collector (PDrC-3000, Yflow, Spain) rotating at 100 rpm was used. The electrospun fibres were collected on aluminium foil and dried at 50 °C, for 24h. After production, the nanofibres were crosslinked by heating at 140 °C for 30 min. The crosslinked fibres were washed with distilled water and dried under vacuum (10 kPa, 50 °C, 24 h) for dendrimer grafting. The stability of crosslinked nanofibers was studied by immersion in water. For it, accurately weighed pieces of crosslinked electrospun membranes were immersed in water. The NPOC (Non-Purgeable Organic Carbon) of the resulting solutions was analysed using a Total Organic Carbon (TOC) analyser and the results expressed as wt% release of soluble substances.

Membrane functionalization by dendrimer grafting

The amine-terminated groups of PAMAM G5-NH_2 were used to attach dendrimers to PAA/PVA fibres via amide formation with their surface carboxyl groups by means of the coupling agent DCC [30, 31]. To check the efficiency of PAMAM G5-NH_2 insertion on membrane fibres, two different amounts of dendrimer were tested using two kinds of fibres with different concentration of carboxyl groups. Reaction conditions and the specific formulation for each sample are given in Table 1. The amount of carboxyl groups per unit mass of dry PAA/PVA membrane was determined by titration as described below. For the functionalization process, accurately weighted pieces of about 100 mg of the dry PAA/PVA base membrane were immersed in a PAMAM G5-NH_2 dendrimer solution in DMF containing DCC with a molar ratio of 1:1 with respect to the available carboxyl groups (7.9 mmol/g and 12.5 mmol/g for 35:65 and 83:17 PAA/PVA formulations respectively). The mixture was kept under constant shaking (100 rpm) for 24 h at room temperature. After amide formation reaction, the membranes were washed with DMF and water and kept for 16 h in distilled water to remove unattached dendrimer molecules, residual reagents and functionalization by-products. Finally, the membranes were vacuum dried at 50 °C for 24h. The amount of dendrimer grafted per gram of the mats was calculated based on the total nitrogen content of the samples.

Thymol loading and migration tests

The dendrimer-modified membranes were loaded with thymol by displacing the ethanol with water from a solution of thymol in ethanol [32-34]. Control experiments were performed using unmodified PAA/PVA membranes. Accurately weighted pieces of approx. 3.5 x 2.5 cm (~ 50 mg) of neat and dendrimer-functionalized PAA/PVA membranes were immersed into 5 mL ethanol solution (75% v/v) containing 50 mg thymol for 20 h at room temperature. After that, water was slowly dropped until a final volume of 20 mL. Finally, all samples were rinsed three times with water and dried at room temperature for 24h. To determine the loading/encapsulation performance, the dry samples were extracted twice with pure ethanol in an orbital shaker. Thymol concentration was measured by UV spectrophotometry at the maximum absorbance of thymol (275 nm) using a freshly prepared calibration curve. A second contact with thymol was performed to assess reusability of PAMAM G5-NH_2 dendrimer-functionalized membranes. To this end, after the total extraction of thymol with ethanol, the membranes were washed with water for 24h, dried at 50 °C, and reloaded with thymol using the same procedure described before.

Migration tests with food contact materials were performed using thymol-loaded PAMAM G5-NH_2 dendrimer-functionalized membranes. The assessments were performed by total immersion into five food simulants, according to European Standard EN 13130-2005 (Materials and articles in contact with foodstuffs. Plastics substances subject to limitation. Guide to test methods for the specific migration of substances from plastics to foods and food simulants and the determination of substances in plastics and the selection of conditions of exposure to food simulants): distilled water, pH 5.6 (A); acetic acid 30 g/L, pH 2.4 (B); and ethanol 100 mL/L, pH 4.0 (C) as aqueous food simulants whereas ethanol 950 mL/L (D) and isooctane (E) were used as non-aqueous fatty food simulants as established as substitutes to olive oil in the Standard EN-13130-1:2004. All simulants were non-buffered, the indicated pH corresponding to the average value along the release experiments indicated below. Samples of approx. 50 mg were immersed in 15 mL of each food simulant in a sealed

vessel that was gently agitated (60 rpm) in an orbital shaker. Thymol migration from controls and thymol-loaded dendrimer-functionalized membranes were monitored until equilibrium at prescribed times: 2 h, 4 h, 6 h, 8 h, 12 h, 24 h, 48 h, 5 d and 15 d. Thymol was analysed by UV spectrophotometry as described before. Neat PAA/PVA membranes were used as reference samples. All experiments were performed in triplicate.

Computational procedure

Thymol was assembled within Discovery Studio, version 2.1, software package, using standard bond lengths and bond angles. With the CHARMM force field [35] and partial atomic charges, the molecular geometry of thymol was energy-minimized using the adopted-based Newton-Raphson algorithm. Structures were considered fully optimized when the energy changes between iterations were less than 0.01 kcal/mol [36]. The initial dendrimer structure was obtained from Maingi et al. using the structure where the terminal amine groups are protonated to mimic PAMAM dendrimer at neutral pH conditions [37]. Docking calculations were performed with the program Autodock Vina [38]. AutoDockTools (ADT; version 1.5.4) was used to add hydrogens and partial charges for dendrimer and ligand using Gasteiger charges. Flexible torsions in the ligand were assigned with the AutoTors module, and the acyclic dihedral angles were allowed to rotate freely. VINA uses rectangular boxes for the docking site therefore, the box centre was defined and the docking box was displayed using ADT.

Table 2. Coordinates of the grid box for blind and focused dockings. (Spacing 1 Å.)

	x center	y center	z center	Size x	Size y	Size z
Blind Docking	53.828	55.365	55.103	74	74	74
Focused docking 1	81.798	59.244	56.748	24	66	22
Focused docking 2	58.898	82.031	50.266	24	30	30
Focused docking 3	80.225	73.258	50.266	24	30	30
Focused docking 4	78.858	41.844	50.266	24	38	38
Focused docking 5	70.543	44.749	77.591	24	44	30
Focused docking 6	28.038	55.749	48.800	32	38	78
Focused docking 7	67.141	51.118	77.003	32	54	30
Focused docking 8	23.811	58.175	56.329	20	28	28
Focused docking 9	60.679	58.175	27.377	20	28	28

The 3-dimensional parameters for docking the ligand to the dendrimer were determined using the GridBox option. The docking procedure was applied to whole dendrimer target, without imposing docking sites. This process is considered as blind docking. For it, the centre of grid box was chosen in such a way that search space for thymol limits to the interior region of PAMAM G5-NH_2 dendrimer. Besides, multiple docking experiments have been used focusing on the dendrimer surface. For blind and focused dockings, the grid centre coordinates, are included in Table 2 with grid points separated 1 Å. Default parameters were used except num_modes, which was set to 40. Thymol was docked 50 times onto the PAMAM-G5 molecule and the docking results generated were directly loaded into Discovery Studio, version 2.1. for their analysis. The best scoring docked conformation was selected in each case.

Analyses

The amount of carboxyl groups per unit mass of membrane was determined by titration. Membrane samples were accurately weighed and protonated using 0.1 M HCl for 24 h, washed with deionized water and immersed in 0.1 M NaOH for 24 h. The resulting solution was titrated with 0.1 M HCl to derive the moles of carboxyl groups per unit mass of dry membrane. The experiments were carried out under nitrogen atmosphere. Total Organic Carbon (TOC) was measured as NPOC (Non-Purgeable Organic Carbon) using a Shimadzu, TOC-VCSH) analyser. The nitrogen content of membrane samples was determined by elemental analysis using a LECO CHNS/O-932 equipment. Surface morphology was studied by using a field emission scanning electron microscope (SEM) operated at 25 kV (DSM-950 Zeiss, Oberkochen, Germany) with gold-coated samples. Attenuated Total Reflectance Fourier Transform Infrared (ATR-FTIR) measurements were taken using a Thermo-Scientific Nicolet iS10 with Smart iTR-Diamond ATR module equipment. The spectra were obtained in the 4000–500 cm^{-1} with a resolution of 4 cm^{-1}. Surface ζ-potential measurements of the modified and unmodified PAA/PVA membranes were performed using dynamic light scattering in a Zetasizer Nano-ZS apparatus equipped with the ZEN 1020 Surface Zeta Potential (Malvern Instruments Ltd., UK). A small membrane piece was glued to the sample holder and inserted into a cuvette containing 10 mM KCl, pH 6.0 with of 0.5 wt% PAA (450 kDa) as tracer. Measurements were performed at 25 °C at six different distances from membrane surface.

Results and discussion

PAMAM G5-NH_2-functionalized PAA/PVA nanofibres

The base PAA/PVA electrospun membranes were stabilized by crosslinking esterification for 30 min at 140 °C, after which they were kept in water until constant weight. The stability of electrospun as revealed by the amount of non-crosslinked materials showed that the two formulations used in this study released < 10 mg NPOC/g membrane (equivalent to < 1 wt%) after 24 h in water and < 0.5 mg NPOC/g membrane (equivalent to < 0.05 wt%) after 48 h. The membranes used in this work were water preconditioned for 48 h, after which no significant release of organic matter took place. The titration of free carboxyl groups yielded 12.5 ± 0.7 and 7.9 ± 0.3 mmol COOH/g of membrane for 83:17 and 35:65 PAA/PVA

DOI: 10.1039/C7TB01498H

membranes respectively (Table 1). Both membranes were used as base material for dendrimer functionalization, which was performed using two different amounts of PAMAM-G5-NH_2. The amount of dendrimer grafted per unit mass of membrane is shown in Table 1 and was larger for 83:17 than 35:65 PAA/PVA base membranes, as expected from their higher amount of carboxyl groups (+4.6 mmol COOH/g membrane). The yield of PAMAM G5-NH_2 increased with the amount of dendrimer in the functionalization solution. Doubling the concentration of dendrimer, the final content of PAMAM G5-NH_2 in the final membranes roughly doubled reaching the maximum value of $2.25 \times 10^{-6} \pm 3.0 \times 10^{-7}$ mmol PAMAM G5-NH_2/mg membrane for G5(+)@83/17 membranes. It has been reported that the stable by-product N-acylurea from the carbodiimide reaction with carboxyl groups formed only in the presence of an excess of carbodiimide [39]. Based on that, we used an equimolar amount of DCC with respect to the carboxyl groups in PAA/PVA membranes. The dicyclohexulurea that could have been formed was removed during the washing process of functionalized membranes as revealed by FTIR spectra. The zeta potential of membrane fibres after grafting PAMAM G5-NH_2 dendrimer were less negative, increasing about 15 mV from the more negative values obtained for neat PAA/PVA membranes. Amine-terminated PAMAM dendrimers bear a positive charge at slightly acidic pH, but the large excess of carboxyl groups in PAA/PVA membranes made them overall negative [40]. The values of surface ζ-potential are listed in Table 3.

Table 3. Surface ζ-potential and thymol loading capacity of PAMAM G5-NH_2 functionalized membranes

Membrane	Surface ζ-potential (mV, pH 6)	Thymol loading 1st charge (mol thymol/g membrane)	Thymol loading 4th charge (mol thymol/g membrane)	PAMAM G5-NH_2 loading (mol thymol /mol G5)
83/17 (Neat)	-44.5 ± 7.6	$4.56 \times 10^{-5} \pm 3 \times 10^{-7}$	$3.84 \times 10^{-5} \pm 1.8 \times 10^{-6}$	-
G5(-)@83/17	-31.1 ± 0.6	$1.20 \times 10^{-4} \pm 3.3 \times 10^{-5}$ (*)	$1.10 \times 10^{-4} \pm 1.7 \times 10^{-5}$ (*)	39 ± 3
G5(+)@83/17	-30.4 ± 0.1	$2.05 \times 10^{-4} \pm 7 \times 10^{-6}$ (*)	$1.94 \times 10^{-4} \pm 1.4 \times 10^{-5}$ (*)	41 ± 4
35/65 (Neat)	-35.2 ± 0.2	$1.84 \times 10^{-5} \pm 2 \times 10^{-7}$	$1.62 \times 10^{-5} \pm 4.7 \times 10^{-6}$	-
G5(-)@35/65	-25.9 ± 6.2	$5.7 \times 10^{-5} \pm 1.8 \times 10^{-5}$ (*)	$5.6 \times 10^{-5} \pm 1.8 \times 10^{-5}$ (*)	31 ± 8
G5(+)@35/65	-22.3 ± 0.4	$1.30 \times 10^{-4} \pm 2.4 \times 10^{-5}$ (*)	$1.36 \times 10^{-4} \pm 2.8 \times 10^{-5}$ (*)	39 ± 4

* difference from the amount adsorbed by neat PAA/PVA membranes

Figure 1 represents the FT-IR spectra of PAA/PVA nanofibres before and after modification with PAMAM G5-NH_2 dendrimer. FTIR spectra of neat PAA/PVA membranes revealed the characteristic peaks associated with PAA and PVA. The broad O–H stretching band (3200-3600 cm^{-1}) appears as the most characteristic feature of alcohols [41]. The C–H alkyl stretching band (2850–3000 cm^{-1}) is also clear as well as the peak at 1142 cm^{-1}, which is attributed to C-O stretching in the crystalline domains of PVA [42]. The characteristic carboxyl stretching frequency of PAA is observed at 1700 cm^{-1}, while the symmetric and antisymmetric stretching frequencies of the carboxylate ion appeared at 1420 and 1560 cm^{-1} [43]. In modified mats, the signals of primary amine N-H stretch at 3320 cm^{-1}, N-H bending at 1550 cm^{-1} and the C=O stretching band from the amides at 1640 cm^{-1} were clearly recognizable. At pH 7 the surface primary amines of PAMAM dendrimers is partly charged as their pK_a is 6.85 [44]. N-H stretch appeared as a shoulder in the broad O-H band in quaternary ammonium dendrimer salts [45]. The increase in the alkyl stretching signal with a clear separation between CH_2 asymmetric stretching band at 2924 cm^{-1} and CH stretching symmetric band at 2848 cm^{-1} is also evidencing the attachment of dendrimers to PAA/PVA fibers. The decrease in the carboxyl signals at 1700 cm^{-1} and 1420 cm^{-1} was consistent with the amide formation reaction. The presence of thymol in electrospun hybrid fibers after encapsulation was also confirmed by FTIR analysis (Fig. S1, Electronic Supplementary Information). A broad band between 3400 and 3100 cm^{-1} corresponded to phenolic OH stretching. The peaks at 1360 and 1241 cm^{-1} can be attributed to OH in-plane bending vibration and C-O stretching in phenol, respectively [46]. The bands at 804 and 738 cm^{-1} were due to out of plane aromatic C-H wagging vibrations [47], while the expected band between 2955 and 2863 cm^{-1} related to CH_3 stretching, was over-lapped with the dominant bands corresponding to CH_3 and CH_2 symmetric and asymmetric stretching vibrations of the base material [48].

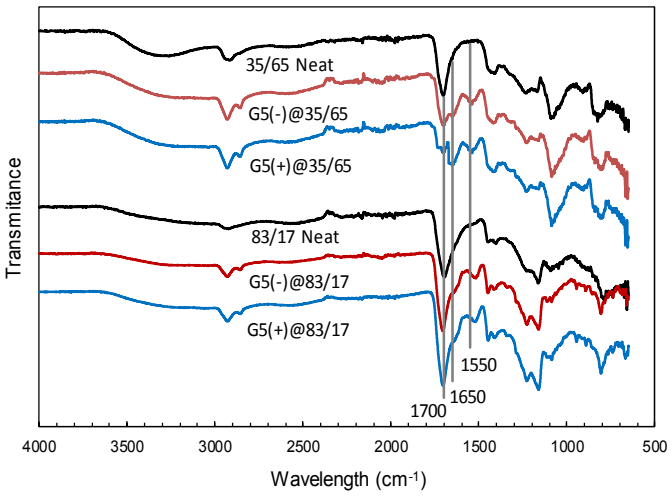

Figure 1. FTIR spectra of neat and PAMAM G5-NH_2-functionalized membranes.

Figure 2 shows SEM micrographs of electrospun 83/17 (A), G5(+)@83/17 (B), 35/65 (C) and G5(+)@35/65 (D) membranes. A and C represent specimens before functionalization while B and D correspond to membranes functionalized with the highest amount of PAMAM G5-NH_2. The average fibre diameter, obtained from SEM micrographs, was 254 ± 65 nm and 320 ± 52 nm for 83/17 and 35/65 membranes, respectively. The fibers were uniform, straight and well-defined without beading or other apparent flaws. After dendrimer functionalization and washing (Figures 2B and 2D) some fibre merging between adjacent fibers at their contact points was observed, but the fibrous morphology of membranes was retained. An additional set of SEM micrographs is presented in Figure S2 (ESI) showing all functionalized membranes unloaded and thymol loaded. No significant differences have been observed between specimens before and after the inclusion of thymol.

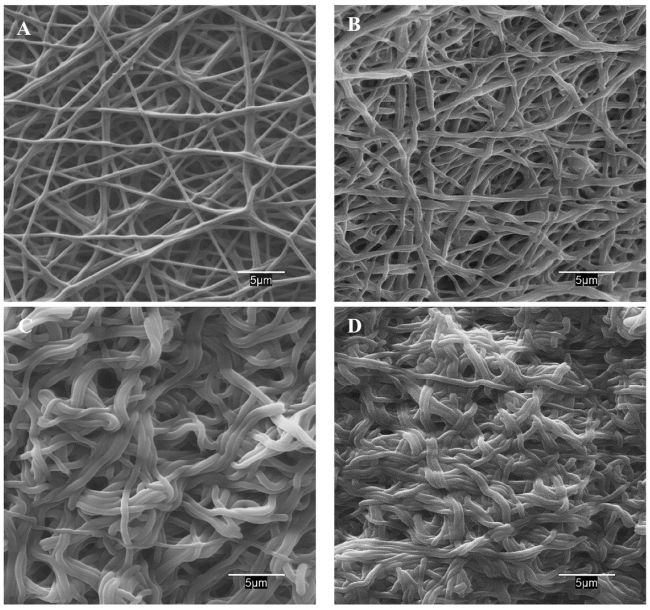

Figure 2. SEM images of PAA/PVA (83/17, A and 35/65, C) membranes and PAMAM G5-NH_2-functionalized membranes G(+)@83/17 (B) and G(+)@35/65 (D).

Thymol loading and release profiles

Table 3 shows the results of the total amount of thymol loaded into neat PAA/PVA and dendrimer-modified membranes. Measurements were performed after four consecutive extractions in ethanol for 24 h at 25°C and ensured the complete removal of thymol from loaded membranes as demonstrated by the absence of thymol in successive re-extractions under the same conditions. A certain amount of thymol was adsorbed on neat PAA/PVA membranes, which accounted for 12-18 % of the total amount of G5(+) membranes, which were those loaded with the higher amount of dendrimer. The most probable reason is the formation of hydrogen bonds due to the existence of numerous carboxylic acid and hydroxyl end groups on membrane surface [49]. The amount of thymol was higher for membranes with higher content of PAMAM G5-NH_2 dendrimer expected. The maximum amount of thymol hosted amounted to 2.05 x 10^{-4} mol thymol/g membrane for G5(+)@83/17 membranes after subtracting the thymol retained by the PAA/PVA base membrane, which was 4.56 x 10^{-5} mol thymol/g membrane. For the whole set of membranes, the hosted amounts (excluding PAA/PVA fibers) were in the 5.7 x 10^{-5}-2.05 x 10^{-4} mol thymol/g membrane range, which corresponded to an average value of 37 molecules of thymol per molecule PAMAM G5-NH_2 with an uncertainty of ± 5 and without significant differences among membrane type and PAMAM-G5-NH_2 loading (Table 3). The recharge capacity of modified membranes was also tested for 4 consecutive recharge assays. The results are shown in Table 3 and Figure S3 (ESI). No statistically significant decline in the thymol loading capacity could be assessed for any of the tested membranes along the 4 cycles of charge-release.

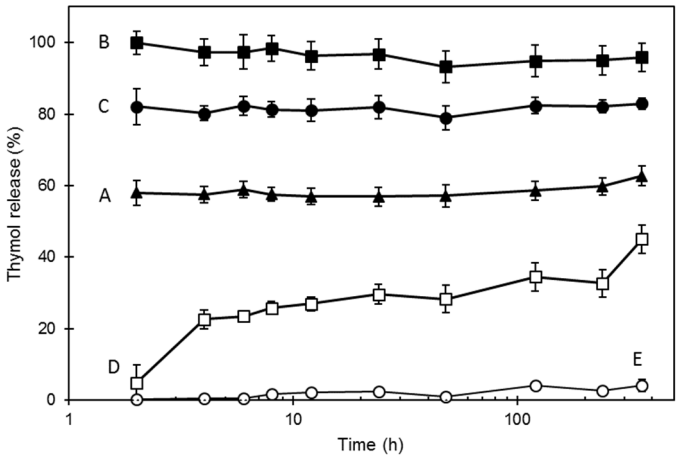

Figure 3. Release of thymol with the time in contact with different media: Water (A), acetic acid 30 g/L (B), ethanol 100 mL/L (C), ethanol 950 mL/L (D) and isooctane (E). The membrane, G5(+)@35/65, was previously loaded with thymol as indicated in Table 3. Thymol concentration was recorded for 15 days, the later point representing 360 h.

Figure 3 presents the percent release of thymol when G5(+)@35/65 membranes, fully loaded with thymol, were put in contact with the five food simulants indicated before. The membrane used for this purpose was based on 35/65 PAA/PVA formulation because in this case thymol loading was below the overall migration limit of 10 mg/dm^2 established by EU Commission Regulation 10/2011). Taking into account the geometry of functionalized membranes, the loading for G5(+)@83/17 was > 30 mg/dm^2, whereas for G5(+)@35/65 the maximum loading was 9.1 mg/dm^2. The difference is most probably due to the lower swelling observed in membranes with higher PAA content [23].

The release of thymol was very rapid at low pH (simulant B) with > 90% of the thymol released before the first measurement (2 h). The extended dendritic conformation and

DOI: 10.1039/C7TB01498H

the weaker character of hydrophobic interactions in acetic acid solution promoted the fast discharge of thymol from the dendrimer hosting sites. In diluted ethanol (simulant C), roughly 20 % of the thymol initially loaded remained after 15 days, the other 80% being released in less than 2 h. Similar behaviour was observed in water (simulant A), but the amount of thymol retained at the end of the assay was higher, about 40%. The higher solubility of thymol in acetic acid and absolute ethanol might be responsible for the variation in the released rate [50]. The protonation of surface amines at low pH and the subsequent loss of its ability to interact with thymol molecules together with the opening of the dendrimer box under acidic conditions would be the reason for the fast release at low pH [51, 52]. In 95 vol% ethanol (simulant D) the release of thymol followed a two-stage profile. After a relatively rapid release during the first 4 h, thymol passed to the solution at an essentially constant rate of ~ 8 x 10^{-4} mmol thymol g membrane^{-1} day^{-1}. Practically no release of thymol was observed in isooctane (simulant E). The loading of thymol on the functionalized membranes is expected to be driven by a combination of hydrogen bonding and hydrophobic interactions [15]. The rapid release phase observed for simulant D, which represented approx. 3.4 x 10^{-5} mol thymol/g membrane in 4 h, could be attributed to the less tightly bound molecules attached to the external surface of the PAA/PVA fibers (~12% of the total amount of thymol) or the external dendritic core. The slow release phase would represent the thymol encapsulated inside dendrimer cavities of forming more stable complexes with the outer functional groups of the dendrimer molecules. At the end of the release and repeated release experiments, the tested mats did not show any apparent loss of capacity.

Computational modelling

The purpose of using molecular modelling to understand PAMAM G5-NH_2 interaction with thymol was to obtain a reliable complex stoichiometry and a suitable binding mode for the ligand-dendrimer association between dendrimer and thymol using docking simulations. Host molecule binding can be the result of both covalent and non-covalent interactions at the surface and in the internal void spaces. The computational approach consists of a blind docking run that covers the complete dendrimer and a set of independent docking runs carried out on small boxes centred on the dendrimer surface (focused docking). For the docking simulations, the initial dendrimer structure chosen was that in which the terminal amine groups are protonated to mimic PAMAM dendrimer at neutral pH conditions. In these conditions, the -OH group of thymol molecules is not ionized and, therefore, the interactions that are established are of the hydrogen bond type and non-electrostatic. The first modelling strategy provided information related to the internal cavities and can be used to estimate the number of host molecules the dendrimer can encapsulate. From the focused docking experiments, the thymol molecules attached onto the dendrimer surface could be estimated. The coordinates containing the information about the size and position of grid box used in blind and focused dockings are tabulated in Table 2.

PAMAM G5-NH_2 was blindly docked with thymol using Autodock Vina. This technique was used to determine appropriate binding sites present in interior of the dendrimer and the whole structure of this is covered under imaginary 3D grid box for docking. Figures 4 and S4 show the docking model of thymol in association with the dendrimer. The results indicated that PAMAM G5-NH_2 dendrimer could accept up to 16 molecules with binding energies calculated by docking score in the (−3.7)-(−4.8) kcal/mol range. This result can be attributed to the interaction of thymol molecules with the hydrophobic internal cavities of PAMAM dendrimers that drive

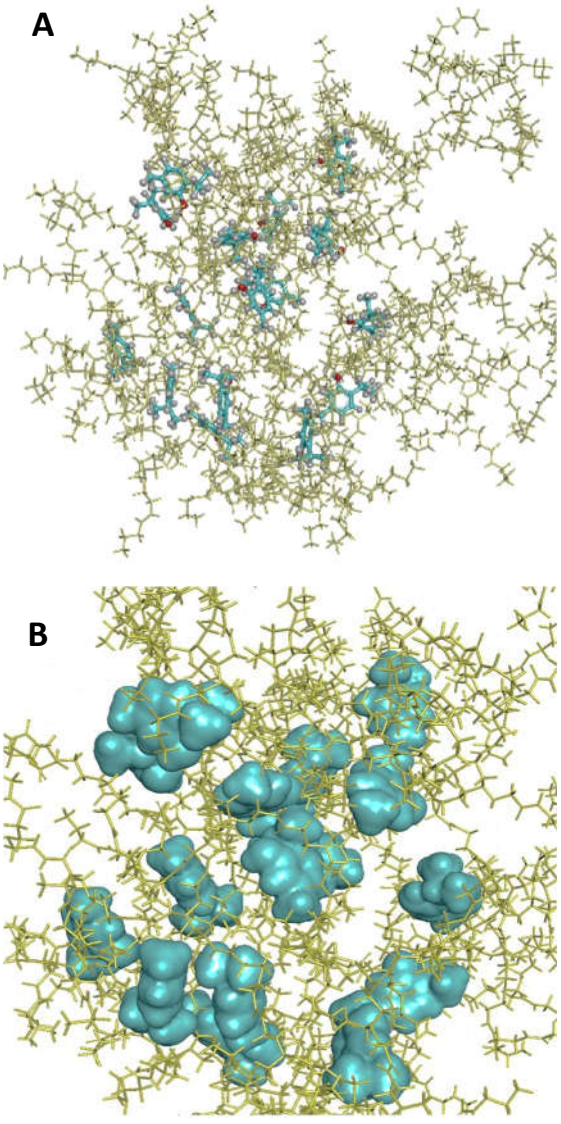

Figure 4. Docking model of thymol molecules (blue) associating to the PAMAM G5-NH_2 dendrimer (yellow). (A) Thymol molecules and dendrimer represented as sticks. (B) Thymol molecules represented as surfaces.

aromatic non-polar molecules to penetrate the dendrimer cages. Thymol molecules were located in protected pocket-like structures formed between or under dendrimer branches. The docking calculations showed that the interaction took place mainly with the hydrophobic parts of the dendrimer plus a minor hydrophilic interaction via hydroxyl groups.

The affinity of the complex involves a hydrophilic and hydrophobic interactions, which are explicitly shown in Figure 5. Hydrophilic interactions come from the formation of hydrogen bonds involving hydroxyl groups of thymol molecules. Hydrophobic interactions involve the phenyl, the methyl and isopropyl groups. This hypothesis is in agreement with previous studies. The location near the tertiary amines and between branches of the dendrimer is the same association site as previously proposed from experiments with other guest molecules including 2-naphthol. Kleinman et al. proposed that the alcohol from 2-naphthol interacts with the tertiary amine of PAMAM dendrimers by hydrogen bonds [53]. Yang et al. showed that one encapsulation site for phenylbutazone was between dendrimer branches near the tertiary amines [54]. In light of these results, the location around the tertiary amine of PAMAM dendrimers appears to be a favourable association site for hydrophobic aromatic groups in general.

PAMAM G5-NH_2 at neutral to slightly acidic pH contains most of the tertiary amines in non-protonated form. The hydroxyl group of the benzene skeleton participates as hydrogen bond acceptor in the interaction with the carbonyl and amino groups located within the dendrimer. One important factor in dendrimer-guest interaction is the location of the guest association sites within the dendrimer structure. At neutral pH conditions, the open structure of the PAMAM G5-NH_2 dendrimer allows 4 thymol molecules to diffuse to locations near the dendrimer centre (Figure S5, ESI). The other 12 molecules of thymol were located near the tertiary amines and between dendrimer branches.

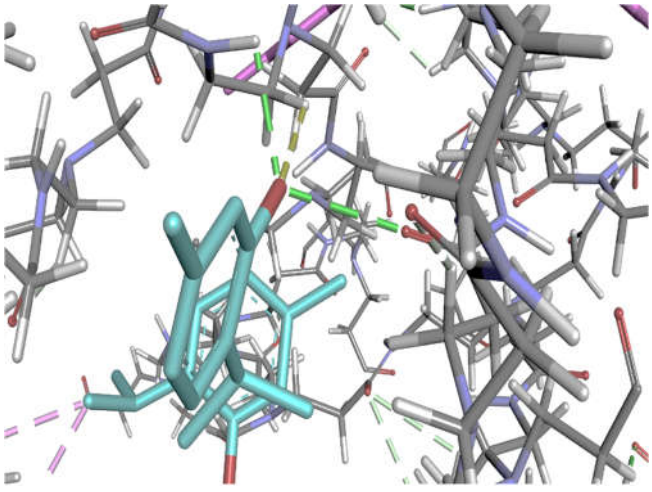

Figure 5. Representation view of the interaction between thymol (blue) and PAMAM-G5 dendrimer, indicating the role of the hydrogen bonds in the capture. Intermolecular hydrogen bonds are drawn as dashed green lines.

Focussed docking experiments determined the number and position of the thymol molecules attached to the periphery of PAMAMG5-NH_2. The results showed that 25 additional thymol molecules could be hosted at the dendrimer surface where the docking contacts involve the outer part or the dendritic branches. Overall, modelling studies showed that 41 (16 + 25) thymol molecules can be hosted either on dendrimer surface and in internal cavities (Figure 6).

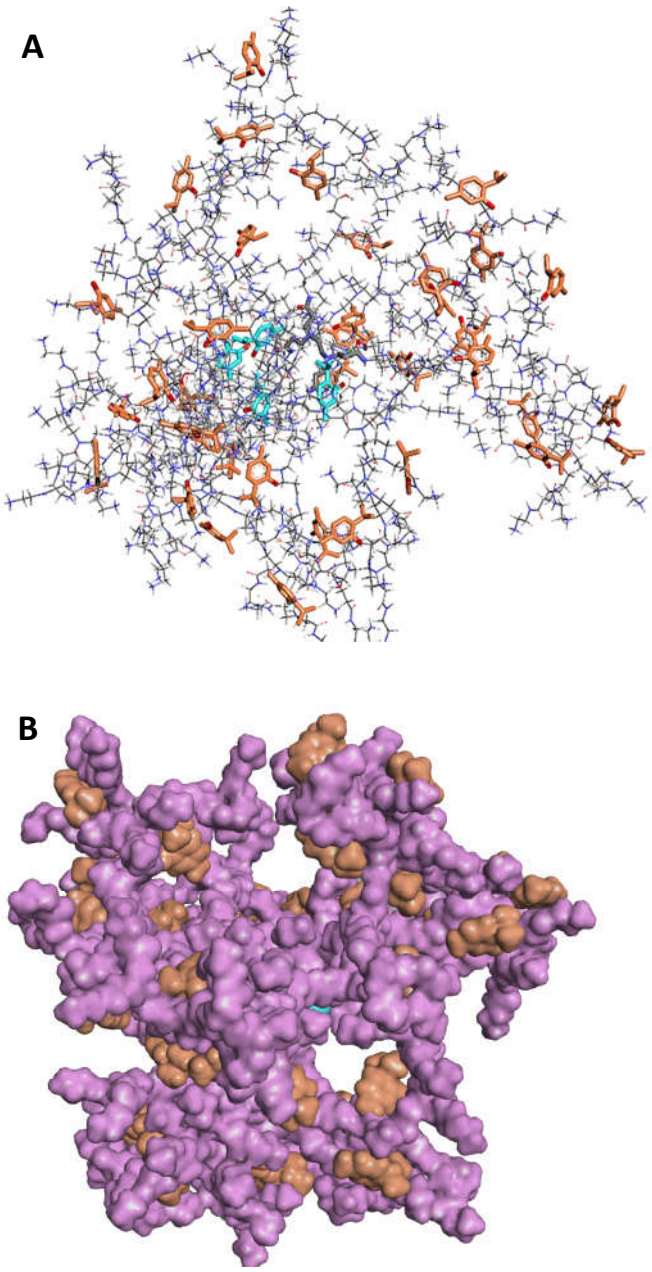

Figure 6. Docking model of the 41 thymol molecules associated to the G5 dendrimer. (A) Thymol molecules and dendrimer represented as sticks. (B) Thymol molecules are represented as blue and orange surfaces and PAMAM-G5 dendrimer pink coloured. (The four thymol molecules located near the dendrimer core were coloured in blue.)

DOI: 10.1039/C7TB01498H

The binding energies showed that the interaction between thymol and dendrimer surface led to less stable complexes than those of thymol encapsulated inside dendritic cavities. The binding energies calculated by the docking score were in the (−2.4)-(−3.4) kcal/mol range, ~ 30% lower than those of thymol in internal cages, but strong enough to explain the experimental results of maximum thymol loading (excluding the amount retained by PAA/PVA fibres) of 35 ± 5 molecules of thymol per molecule of PAMAM G5-NH_2 (Table 3). In diluted ethanol (simulant C), the thymol retained in the membrane after 15 days, would correspond to the molecules encapsulated inside the dendrimer, representing about 35% of the total amount of thymol, plus the more tightly ones hosted in the outer parts of the dendrimer molecule. The difference between simulants A and C can be explained by the higher pH of the former, which resulted in a tighter dendritic conformation. The behaviour with non-aqueous fatty food simulants is significant, as it represents an improvement over many active agent carriers that generally suffer from a severe burst release in fatty simulants [55-57].

PAMAM dendrimers have a large number of cationic surface groups. The pKa of primary amines in the outer layer of PAMAM dendrimers is in the 9.0-10.8 range [58]. Consequently, surface protonated amines of PAMAM G5-NH_2 offer binding sites for hydrogen bonds with thymol molecules [59]. The internal tertiary amines of PAMAM G5-NH_2 do not undergo complete protonation at slightly acidic conditions, due to their weaker basic character [60]. Their corresponding pK_a was reported in the 5.8-6.7 range [58, 61]. Consequently, the hydrogen bonding of thymol to the surface of PAMAM G5-NH_2 would be favoured in all cases at the pH (6.0 ± 0.5) of the loading thymol-ethanol solution [62]. At the same time, the electrostatic repulsions (excluded-volume interactions and Coulombic repulsions) between the protonated primary and tertiary amines increase the radius of gyration stretches out of dendritic branches, which makes the internal hydrophobic cavities more accessible to thymol molecules [13, 63].

These findings were in a good agreement with the results reported by Buczkowski et al., who studied the interactions of 5-fluorouracil with PAMAM G5-NH_2 and PAMAM G5-OH dendrimers [60]. The authors determined that PAMAM G5-NH_2 is able to guest about 70 5-fluorouracil molecules, three times more than its hydroxyl PAMAM G5-OH counterpart. This fact confirms the importance of the interaction with surface amine groups for the host-guest association of ligand molecules to dendrimers. The interaction with internal tertiary amine groups would be playing a minor role. However, the more hydrophobic interior cavities can retain the thymol molecules with higher binding energy than the dendrimer surface [64].

Conclusions

We prepared electrospun membranes from blends of poly(acrylic acid) and poly(vinyl alcohol), which were stabilized by esterification crosslinking and functionalized by covalent bonding of amino terminated poly(amidoamine) fifth generation dendrimers (PAMAM G5-NH_2). The purpose was to use the membranes for the host-guest encapsulation of the antioxidant thymol.

The electrospun membranes consisted of uniform, straight and well-defined fibers that preserved their fibrous morphology after washing and functionalization. The amount of grafted dendrimer reached 2.25 x 10^{-6} ± 3.0 x 10^{-7} mmol PAMAM G5-NH2/mg membrane and was higher for membranes with higher content of poly(acrylic acid).

The amount of thymol loaded reached a maximum of 2.51 x 10^{-4} mol thymol/g membrane, from which 4.56 x 10^{-5} mol thymol/g membrane corresponded to the PAA/PVA base membrane. For the whole set of membranes, the amount of thymol hosted by the dendrimer represented an average of 37 ± 5 molecules of thymol per molecule PAMAM G5-NH_2. The membranes could be recharged without losing capacity.

Computational modelling allowed determining the molecular details of the dendrimer-guest complex and the calculation of the number of loaded molecules. The results predicted 16 thymol molecules encapsulated around the dendrimer core or between dendrimer branches via hydrophobic interactions. 25 additional thymol molecules could be hosted at the dendrimer surface, although with lower binding energies than those encapsulated inside the dendritic cavities.

Upon contact between thymol-loaded membranes and food simulants, we showed that the release behaviour was mainly driven by the pH of the medium, which determines the opening of the dendrimer box upon amine protonation. In 95 vol% ethanol the release of thymol took place at a relatively constant rate of ~ 8 x 10^{-4} mmol thymol g membrane^{-1} day^{-1} after an initial release of the less tightly bound thymol molecules.

Acknowledgements

Financial support for this work was provided by the FP7-ERA-Net Susfood, 2014/00153/001, the Spanish Ministry of Economy and Competitiveness, CTM2013-45775 and the Dirección General de Universidades e Investigación de la Comunidad de Madrid, Research Network S2013/MAE-2716. GA thanks the University of Alcalá for the award of pre-doctoral grants. The authors wish to thank Carmen García-Ruiz, from the Department of Analytical Chemistry of the University of Alcalá, for her help with ATR-FTIR measurements.

References

1. J. Quirós, K. Boltes and R. Rosal, *Polymer Reviews*, 2016, **56**, 631-667.
2. P. K. Bhattacharjee and G. C. Rutledge, in *Comprehensive Biomaterials*, 2011, vol. 1, pp. 497-512.

3. G. Bruni, L. Maggi, L. Tammaro, R. Lorenzo, V. Friuli, S. D'Aniello, M. Maietta, V. Berbenni, C. Milanese, A. Girella and A. Marini, *International Journal of Pharmaceutics*, 2016, **511**, 190-197.
4. R. Sridhar, R. Lakshminarayanan, K. Madhaiyan, V. Amutha Barathi, K. H. C. Lim and S. Ramakrishna, *Chemical Society Reviews*, 2015, **44**, 790-814.
5. W. Cui, M. Qi, X. Li, S. Huang, S. Zhou and J. Weng, *International Journal of Pharmaceutics*, 2008, **361**, 47-55.
6. J. Zeng, L. Yang, Q. Liang, X. Zhang, H. Guan, X. Xu, X. Chen and X. Jing, *Journal of Controlled Release*, 2005, **105**, 43-51.
7. H. Jiang, L. Wang and K. Zhu, *Journal of Controlled Release*, 2014, **193**, 296-303.
8. Z. Aytac, S. I. Kusku, E. Durgun and T. Uyar, *Materials Science and Engineering: C*, 2016, **63**, 231-239.
9. F. Vögtle, G. Richardt and N. Werner, *Dendrimer Chemistry: Concepts, Syntheses, Properties, Applications*, 2009.
10. E. Abbasi, S. F. Aval, A. Akbarzadeh, M. Milani, H. T. Nasrabadi, S. W. Joo, Y. Hanifehpour, K. Nejati-Koshki and R. Pashaei-Asl, *Nanoscale Research Letters*, 2014, **9**, 247-247.
11. D. Astruc, E. Boisselier and C. Ornelas, *Chemical Reviews*, 2010, **110**, 1857-1959.
12. M. Malkoch, E. Malmström and A. M. Nyström, in *Polymer Science: A Comprehensive Reference, 10 Volume Set*, 2012, vol. 6, pp. 113-176.
13. P. K. Maiti, T. Çağın, S. T. Lin and W. A. Goddard, *Macromolecules*, 2005, **38**, 979-991.
14. E. M. M. Valle, *Process Biochemistry*, 2004, **39**, 1033-1046.
15. S. Khaliliazar, S. Akbari and M. H. Kish, *Applied Surface Science*, 2016, **363**, 593-603.
16. A. Wattanasatcha, S. Rengpipat and S. Wanichwecharungruang, *International Journal of Pharmaceutics*, 2012, **434**, 360-365.
17. K. K. Kuorwel, M. J. Cran, K. Sonneveld, J. Miltz and S. W. Bigger, *LWT - Food Science and Technology*, 2013, **50**, 432-438.
18. M. Ramos, A. Beltrán, M. Peltzer, A. J. M. Valente and M. C. Garrigós, *LWT - Food Science and Technology*, 2014, **58**, 470-477.
19. A. Torres, J. Romero, A. Macan, A. Guarda and M. J. Galotto, *The Journal of Supercritical Fluids*, 2014, **85**, 41-48.
20. T. A. Gill, J. Li, M. Saenger and S. R. Scofield, *Journal of Applied Microbiology*, 2016, **121**, 1103-1116.
21. Y. Wu, Y. Luo and Q. Wang, *LWT - Food Science and Technology*, 2012, **48**, 283-290.
22. J. M. López-Nicolás, P. Rodríguez-Bonilla and F. García-Carmona, *Critical Reviews in Food Science and Nutrition*, 2014, **54**, 251-276.
23. J. Santiago-Morales, G. Amariei, P. Letón and R. Rosal, *Colloids and Surfaces B: Biointerfaces*, 2016, **146**, 144-151.
24. J. L. Drury and D. J. Mooney, *Biomaterials*, 2003, **24**, 4337-4351.
25. N. A. Peppas and D. Tennenhouse, *Journal of Drug Delivery Science and Technology*, 2004, **14**, 291-297.
26. C. R. Nuttelman, D. J. Mortisen, S. M. Henry and K. S. Anseth, *Journal of Biomedical Materials Research Part A*, 2001, **57**, 217-223.
27. S. D. Lee, G. H. Hsiue, P. C. T. Chang and C. Y. Kao, *Biomaterials*, 1996, **17**, 1599-1608.
28. B. Gupta, C. Plummer, I. Bisson, P. Frey and J. Hilborn, *Biomaterials*, 2002, **23**, 863-871.
29. G. Gratzl, S. Walkner, S. Hild, A. W. Hassel, H. K. Weber and C. Paulik, *Colloids and Surfaces B: Biointerfaces*, 2015, **126**, 98-105.
30. T. G. Kim and T. G. Park, *Biotechnology Progress*, 2006, **22**, 1108-1113.
31. J. M. Goddard and J. H. Hotchkiss, *Progress in Polymer Science*, 2007, **32**, 698-725.
32. J. F. Jansen, E. M. de Brabander-van den Berg and E. W. Meijer, *Science (New York, N.Y.)*, 1994, **266**, 1226-1229.
33. A. Sansukcharearnpon, S. Wanichwecharungruang, N. Leepipatpaiboon, T. Kerdcharoen and S. Arayachukeat, *International Journal of Pharmaceutics*, 2010, **391**, 267-273.
34. A. Wattanasatcha, S. Rengpipat and S. Wanichwecharungruang, *International Journal of Pharmaceutics*, 2012, **434**, 360-365.
35. B. R. Brooks, R. E. Bruccoleri, B. D. Olafson, D. J. States, S. Swaminathan and M. Karplus, *Journal of Computational Chemistry*, 1983, **4**, 187-217.
36. A. Morreale, F. Maseras, I. Iriepa and E. Gálvez, *Journal of Molecular Graphics and Modelling*, 2002, **21**, 111-118.
37. V. Maingi, V. Jain, P. V. Bharatam and P. K. Maiti, *Journal of computational chemistry*, 2012, **33**, 1997-2011.
38. O. Trott and A. J. Olson, *Journal of Computational Chemistry*, 2010, **31**, 455-461.
39. E. Valeur and M. Bradley, *Chemical Society Reviews*, 2009, **38**, 606-631.
40. I. J. Suarez, R. Rosal, A. Rodriguez, A. Ucles, A. R. Fernandez-Alba, M. D. Hernando and E. García-Calvo, *TrAC Trends in Analytical Chemistry*, 2011, **30**, 492-506.
41. S. A. Nouh and R. A. Bahareth, *Radiation Effects and Defects in Solids*, 2013, **168**, 274-285.
42. H. S. Mansur, R. L. Oréfice and A. A. P. Mansur, *Polymer*, 2004, **45**, 7193-7202.
43. L. J. Kirwan, P. D. Fawell and W. van Bronswijk, *Langmuir*, 2003, **19**, 5802-5807.
44. D. A. Tomalia, A. M. Naylor and W. A. Goddard, *Angewandte Chemie International Edition in English*, 1990, **29**, 138-175.
45. S. Charles, N. Vasanthan, D. Kwon, G. Sekosan and S. Ghosh, *Tetrahedron Letters*, 2012, **53**, 6670-6675.
46. M. J. Mohammed and F. A. Al-Bayati, *Phytomedicine*, 2009, **16**, 632-637.
47. H. Schulz, G. Özkan, M. Baranska, H. Krüger and M. Özcan, *Vibrational Spectroscopy*, 2005, **39**, 249-256.
48. D. Markovic, S. Milovanovic, M. Radetic, B. Jokic and I. Zizovic, *The Journal of Supercritical Fluids*, 2015, **101**, 215-221.
49. M. Masoumi and M. Jahanshahi, *Advances in Polymer Technology*, 2016, **35**, 221-227.
50. P. Zhu, Y. Chen, J. Fang, Z. Wang, C. Xie, B. Hou, W. Chen and F. Xu, *The Journal of Chemical Thermodynamics*, 2016, **92**, 198-206.
51. J. F. Jansen, E. W. Meijer and E. M. M. de Brabander-van den Berg, *Journal of the American Chemical Society*, 1995, **117**, 4417-4418.
52. R. Esfand and D. A. Tomalia, *Drug Discovery Today*, 2001, **6**, 427-436.

DOI: 10.1039/C7TB01498H

53. M. H. Kleinman, J. H. Flory, D. A. Tomalia and N. J. Turro, *The Journal of Physical Chemistry B*, 2000, **104**, 11472-11479.
54. W. Yang, Y. Li, Y. Cheng, Q. Wu, L. Wen and T. Xu, *Journal of Pharmaceutical Sciences*, 2009, **98**, 1075-1085.
55. C. Gomes, R. G. Moreira and E. Castell-Perez, *Journal of Food Science*, 2011, **76**, N16-N24.
56. S. F. Hosseini, M. Zandi, M. Rezaei and F. Farahmandghavi, *Carbohydrate Polymers*, 2013, **95**, 50-56.
57. Y. Zhang, Y. Niu, Y. Luo, M. Ge, T. Yang, L. Yu and Q. Wang, *Food Chemistry*, 2014, **142**, 269-275.
58. M. S. Diallo, S. Christie, P. Swaminathan, L. Balogh, X. Shi, W. Um, C. Papelis, W. A. Goddard and J. H. Johnson, *Langmuir*, 2004, **20**, 2640-2651.
59. J. Hu, Y. Cheng, Y. Ma, Q. Wu and T. Xu, *The Journal of Physical Chemistry B*, 2009, **113**, 64-74.
60. A. Buczkowski, T. Olesinski, E. Zbicinska, P. Urbaniak and B. Palecz, *International Journal of Pharmaceutics*, 2015, **490**, 102-111.
61. D. Cakara, J. Kleimann and M. Borkovec, *Macromolecules*, 2003, **36**, 4201-4207.
62. Y. Cheng, H. Qu, M. Ma, Z. Xu, P. Xu, Y. Fang and T. Xu, *European Journal of Medicinal Chemistry*, 2007, **42**, 1032-1038.
63. P. K. Maiti, T. Çağın, G. Wang and W. A. Goddard, *Macromolecules*, 2004, **37**, 6236-6254.
64. A. Asthana, A. S. Chauhan, P. V. Diwan and N. K. Jain, *AAPS PharmSciTech*, 2005, **6**, E536-E542.

Electronic Supplementary Information

Poly(amidoamine) dendrimers grafted on electrospun poly(acrylic acid)/poly(vinyl alcohol) membranes for host-guest encapsulation of the antioxidant thymol

Georgiana Amariei[a], Karina Boltes[a], Pedro Letón[a], Isabel Iriepa[b], Ignacio Moraleda[b], Roberto Rosal[a,†]

[a] Department of Chemical Engineering, University of Alcalá, E-28871 Alcalá de Henares, Madrid, Spain.
[b] Department of Organic Chemistry and Inorganic Chemistry, School of Biology, Environmental Sciences and Chemistry, University of Alcalá, E-28871 Alcalá de Henares, Madrid, Spain.
[†] corresponding author: roberto.rosal@uah.es

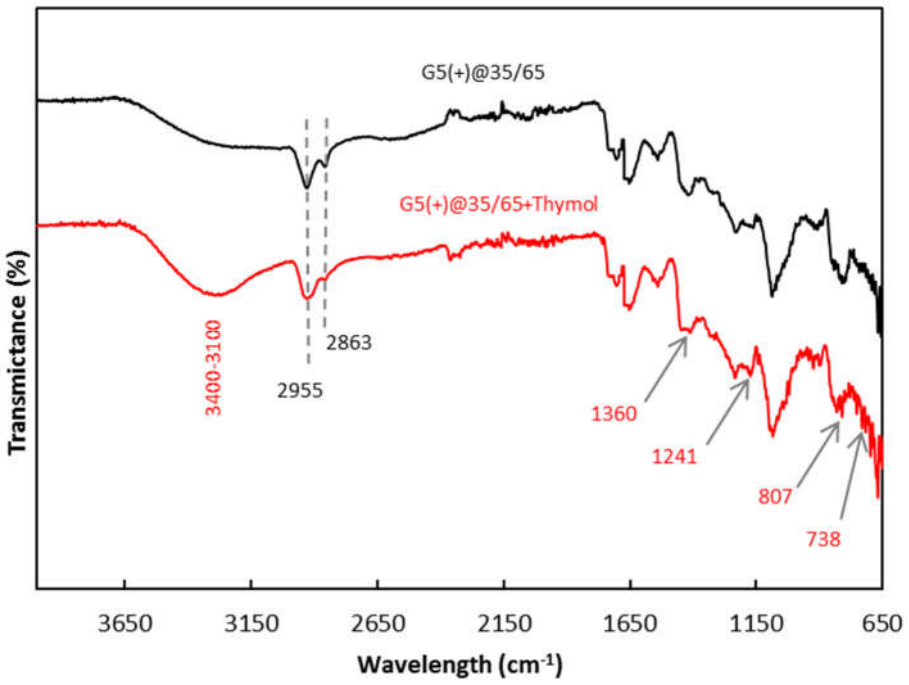

Figure S1: FTIR spectra of 35/65 PAMAM G5-NH2-functionalized membranes before and after thymol loading.

DOI: 10.1039/C7TB01498H

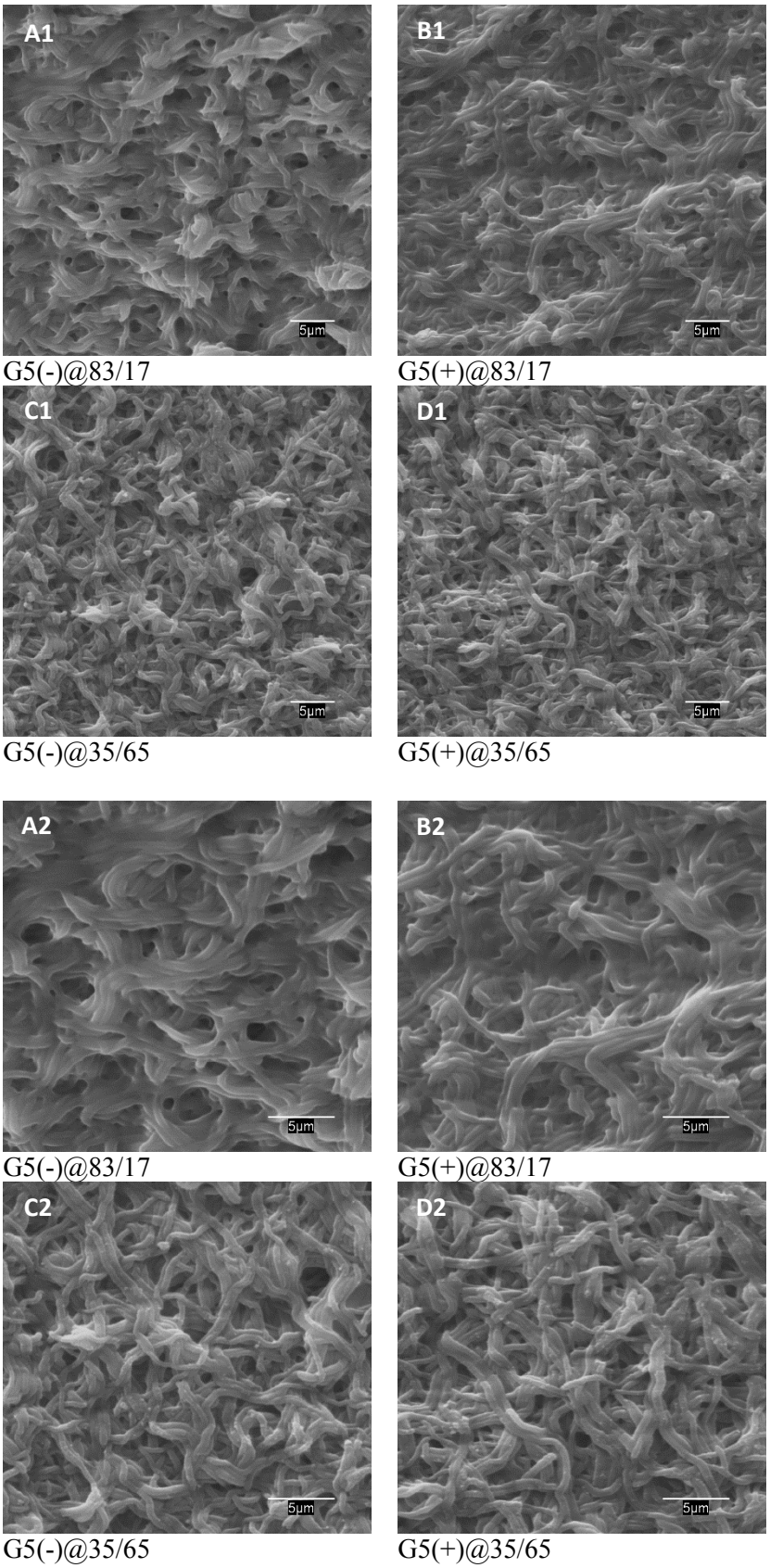

Figure S2. SEM images of PAMAM G5-NH2-functionalized membranes before (A1-D1) and after (A2-D2) thymol loading.

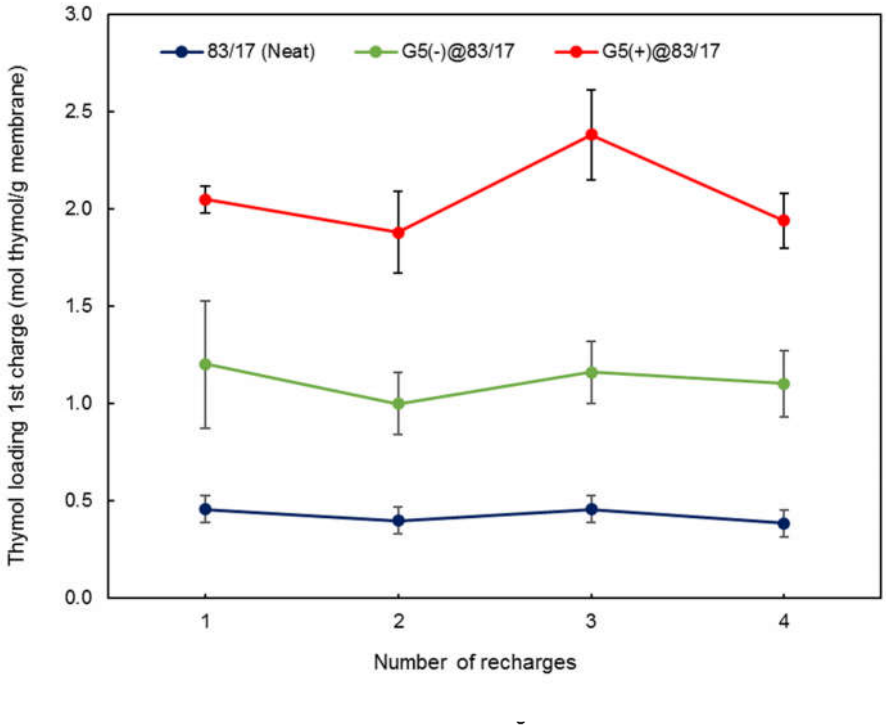

Figure S3. Thymol loading capacity of PAMAM G5-NH2 functionalized membranes after four consecutive charges.

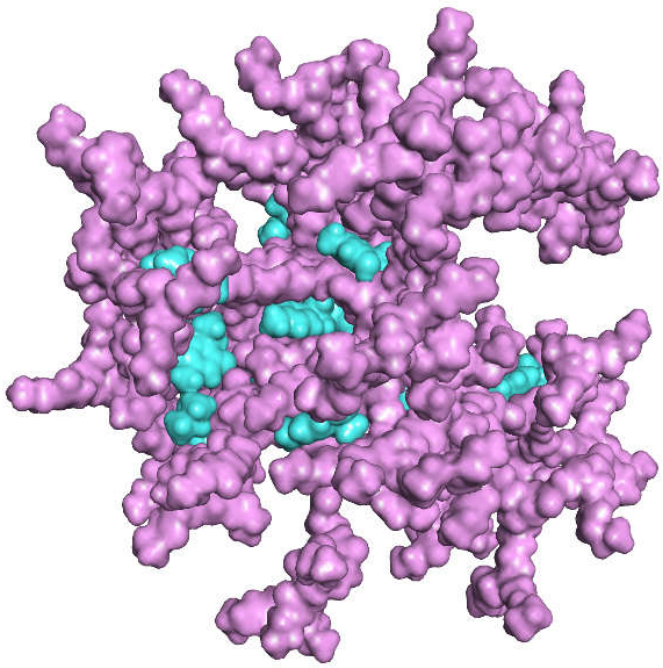

Figure S4. Surfaces of thymol molecules (blue) encapsulated in PAMAM-G5 dendrimer (pink).

DOI: 10.1039/C7TB01498H

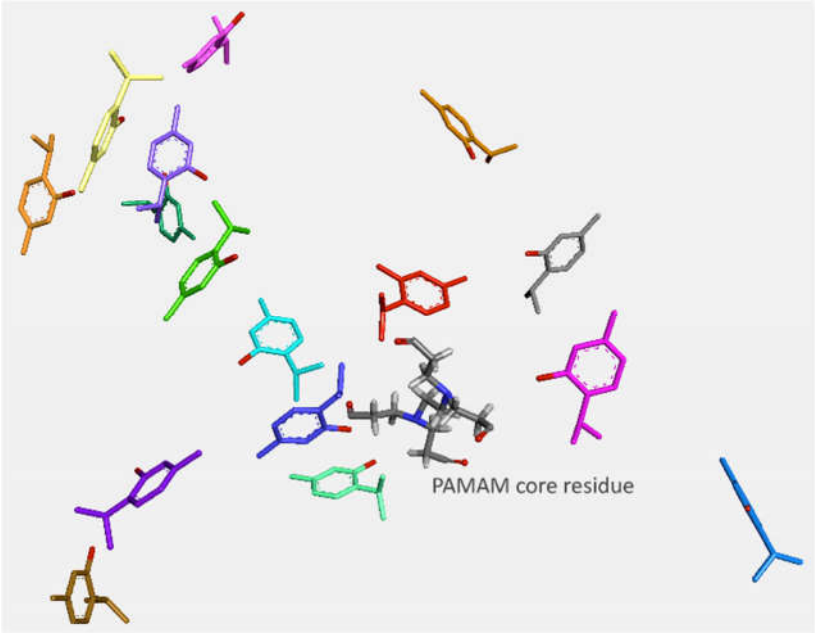

Figure S5. Thymol molecules associated to the G5 dendrimer. The dendrimer centre is shown in sticks and coloured by element. Four thymol molecules coloured in red, turquoise, blue, and light green locate near the dendrimer centre. The other (12) thymol molecules locate in the mid- and outer-regions of the dendrimer.